Michel Electron Reconstruction Using the MicroBooNE LArTPC Cosmic Data

The MicroBooNE Collaboration

August 25, 2016

Abstract

MicroBooNE is a Liquid Argon Time Projection Chamber (LArTPC) neutrino detector located in the Booster Neutrino Beamline at Fermilab which began collecting neutrino data in October 2015. MicroBooNE aims to explore the low-energy excess in the ν_e spectrum reported by MiniBooNE as well as perform ν-Ar cross-section measurements. In this note, we present the current status of reconstructing Michel electrons from cosmic-ray muons in the MicroBooNE detector. These Michel electrons are distributed uniformly inside the detector, and serve as a natural and powerful sample to study the detector's response for low-energy (tens of MeV) interactions as a function of position. We have developed a reconstruction software tool to successfully identify such Michel electrons which could benefit any LArTPC experiment generically.

1 Introduction

The MicroBooNE experiment is a Liquid Argon Time Projection Chamber (TPC) sitting in the Booster Neutrino Beam (BNB) line at the Fermi National Accelerator Laboratory. MicroBooNE aims to study neutrino interactions at the $\mathcal{O}$(1 GeV) energy scale. The TPC can record neutrino interactions by collecting the ionization charge produced by charged particles traversing the detector volume. This charge drifts in a uniform electric field towards wires on which the moving charge induces a current, recorded as a digitized signal. MicroBooNE's TPC consists of three wire-planes, each containing wires separated by 3 mm. As charge drifts towards the anode it first encounters two wire-planes, oriented at +/- 60° with respect to the vertical direction. Charge drifting past these planes induces a current which produces a bi-polar signal in the electronics. These two planes are referred to as induction planes. The wire plane furthest from the cathode has wires oriented verically. Drifting electrons are collected on this plane producing a unipolar signal. This is referred to as the collection plane. Charge deposited in the TPC will produce a 2D inprint in (wire,time) coordinates on a plane. Each plane is a different 2D projection of the same 3D information, and the information from the three planes can be combined to reconstruct a 3D image of the interaction.

The MicroBooNE TPC is a parallelepiped of 2.56×2.32×10.36 meters in the x (in the drift direction), y (vertical coordinate), and z (beam-direction) coordinates respectively. The drift-field is set at 273 V/cm, which leads to a drift-velocity of approximately 11 cm / 100 μs. This slow drift-velocity, compared to the 2.2 μs lifetime for muons [1], means it is challenging to separate charge deposited by the muon and Michel electron respectively based on the arrival time alone, without employing a topological-based reconstruction algorithm. Fig. 1 shows a schematic of the MicroBooNE TPC, its coordinate system, and how it operates. More information on the MicroBooNE detector can be found in the MicroBooNE Technical Design Report [2].

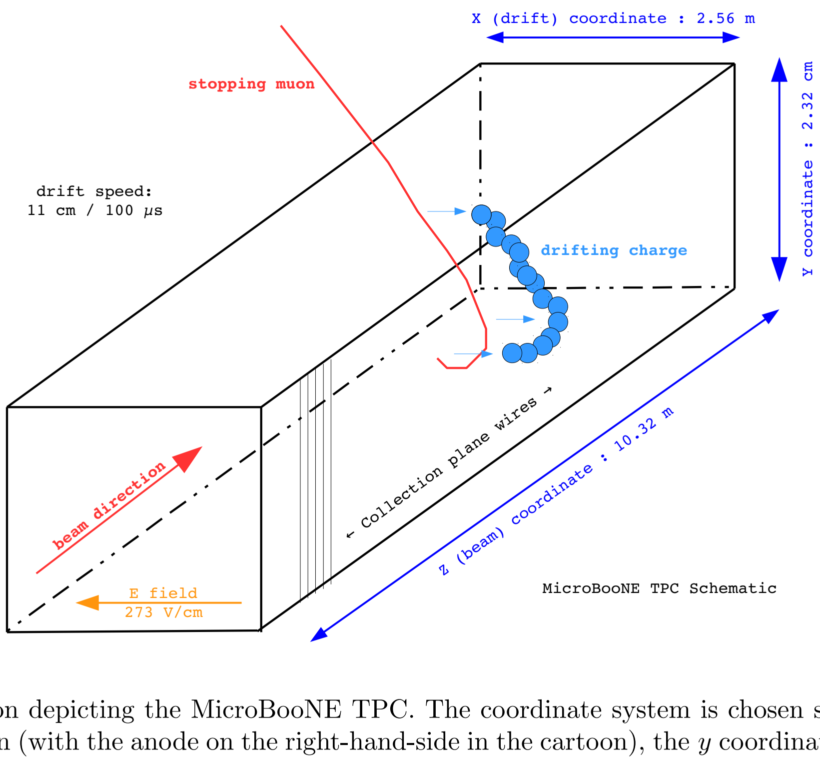

Figure 1: Cartoon depicting the MicroBooNE TPC. The coordinate system is chosen such that x is in the drift-direction (with the anode on the right-hand-side in the cartoon), the y coordinate represents the vertical direction, centered in the middle of the TPC and with the positive coordinate pointing upwards, and the beam-coordinate (z) points in the direction of the beam, starting at the upstream end of the TPC. Ionization charge deposited in the TPC by charged particles will drift towards the wire-planes due to a uniformly applied 273 V/cm drift-field. The drift velocity at such a voltage is approximately 11 cm / 100 μs.

While the MicroBooNE detector is designed to study neutrino interactions, its location on the surface combined with the relatively long readout time (4.8 ms compared to the 1.6 μs BNB beam-spill) causes a large amount of cosmic-ray muons to enter and deposit energy in the detector within the readout window. Some of these muon tracks will stop in the TPC, possibly decaying, producing an electron. Muon decay is a well studied physical process in which a muon decays according to Eq. 1.

$$\mu^- \, (\mu^+) \rightarrow e^- \, (e^+) + \nu_\mu \, (\bar{\nu}_\mu) + \bar{\nu}_e \, (\nu_e) \tag{1}$$

Electrons produced via muon decay at rest are referred to as Michel electrons and have a very well defined energy spectrum which has a sharp cutoff at half the muon mass (105.66 MeV [1]). Fig. 2 shows the Michel electron energy spectrum measured using a beam produced by the Nevis laboratories cyclotron (Ref. [3]).

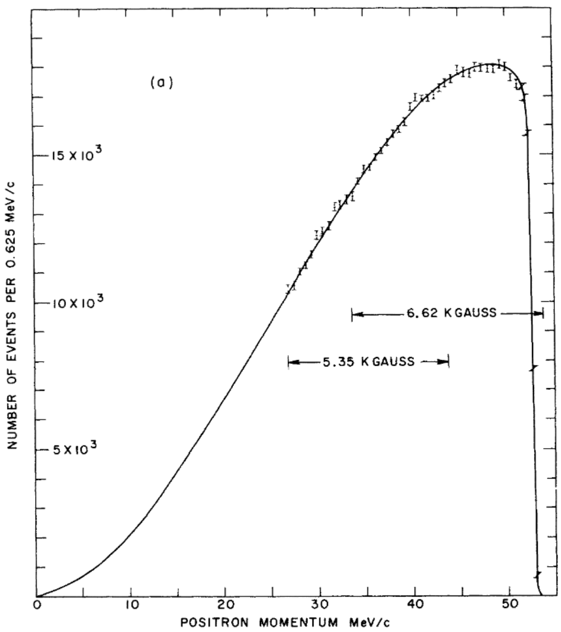

Figure 2: Reconstructed Momentum spectrum of positrons from decay-at-rest muons produced by a positive pion beam from the Columbia University cyclotron at the Nevis laboratories [3].

There are several reasons that motivate us to reconstruct and study Michel electrons produced in the MicroBooNE TPC:

- **Detector Response**: Michel electrons, with their characteristic energy spectrum, can serve as a tool to study the detector response to electrons in the tens of MeV energy range. Specifically, they can be used to study MicroBooNE's energy resolution and identification ability for very low energy Electro-Magnetic (EM) showers.

- **Muon Tagging**: tagging Michel electrons can be useful to perform particle identification, and thus help in the reconstruction of neutrino interactions.

- **Stopping Muon Identification**: Michel electrons can be used to tag stopping muons and therefore differentiate between entering and exiting muon tracks.

Identifying Michel electrons is therefore a useful excercise both as a way to study and understand the detector at this initial stage in the data-taking, as well as a powerful additional discriminant that can help identify and profile stopping muons, which can positively impact future LArTPC neutrino measurements.

We have developed a 2D Michel electron tagging algorithm that relies only on TPC information from a single plane. Furthermore, this algorithm only necessitates simple hit reconstruction and hit clustering algorithms to be used. Our strategy in tagging Michel electrons relies on trying to identify the Bragg peak of a muon track in the detector, followed by a kink in the spatial arrangement of the hits, indicating the presence of a new particle (the Michel electron) being produced after a muon comes to a stop in the TPC. An example event display, showing collection plane raw data associated with a candidate Michel electron is shown in Fig. 3. In this image we can see the two features that we try and pick out: the increased ionization due to the Bragg peak at the end of the muon track, and the large kink indicating a Michel electron produced at a large angle with respect to the muon. We have focused our efforts towards developing an algorithm able to tag Michel electrons with high purity.

In Sec. 2 we present an overview of energy deposition in argon for electrons in the 10-50 MeV energy range. Sec. 3 briefly describes the data-samples used for this work. A more detailed description of the algorithm developed can be found in Sec. 4.

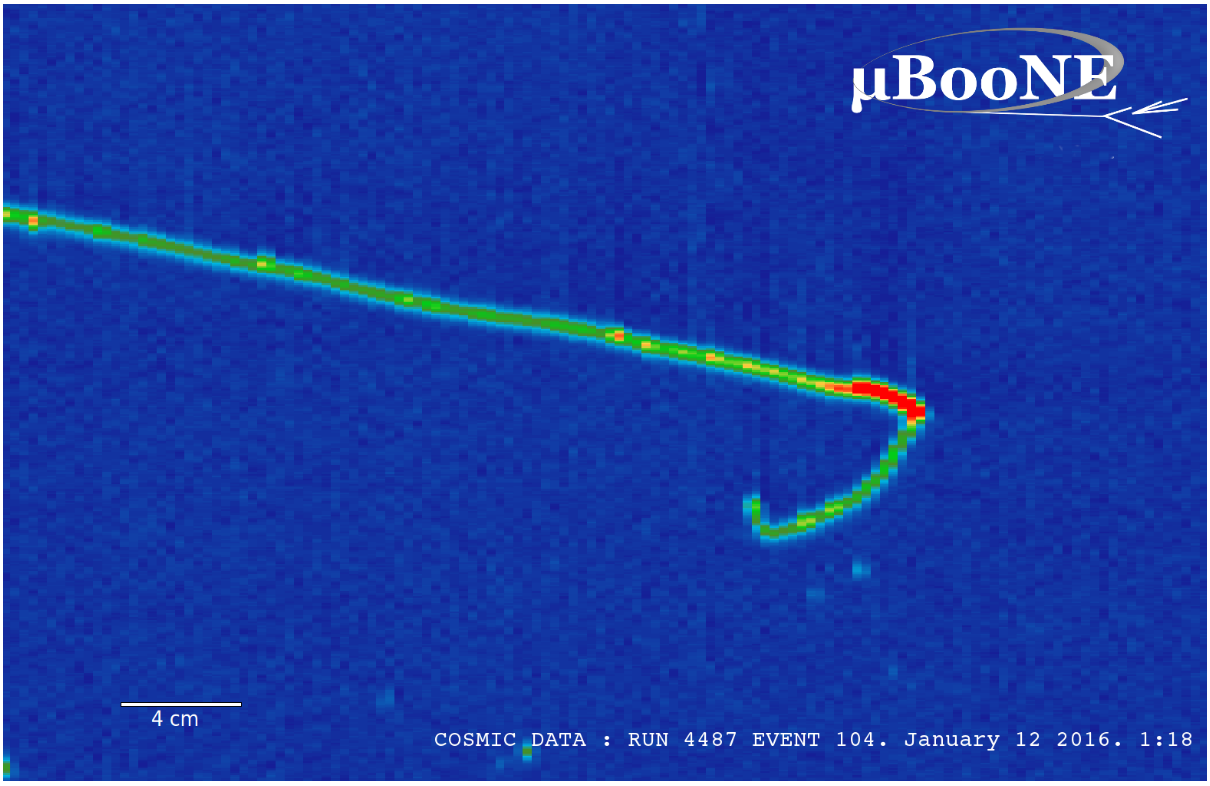

Figure 3: Event display showing raw data for a region of the collection plane associated with a candidate Michel electron. Wire-number is represented on the horizontal axis, and time on the vertical. Color is associated with the ADC count on each channel.

The next step in our reconstruction effort is producing a Michel energy spectrum by estimating the energy response in the detector. To accomplish this we focus on calculating the electronics gain for the TPC wires, and correcting for physics effects such as the electron-lifetime and recombination. We finally produce a reconstructed Michel energy spectrum. Our efforts to reconstruct the Michel electron energy are presented in Sec. 5.

Finally, in Sec. 6 we provide concluding remarks summarizing this work.

2 Michel Electron Energy Deposition in Liquid Argon

Michel electrons are detected by the MicroBooNE TPC because of the energy they deposit as ionization electrons as they travel through the TPC. To identify Michel electrons and reconstruct their energy it is important to understand exactly what signature the electron will leave. In this section we explore the topological mark left by electrons in the tens of MeV energy range in a LArTPC. We specifically try to address through which physical processes do electrons lose energy in the TPC, as well as how much of an electron's energy is lost to ionization electrons. Ultimately we are interested in determining how this will impact the reconstruction of a Michel electron's energy.

Figure 4 shows the stopping power of electrons in argon, as reported by the National Institute of Standards and Technology (NIST). The figure shows the "Collision" and "Radiative" contributions to the stopping power, where the first denotes the energy lost to electron ionization, and the second that which is lost to radiated photons. This figure shows that in the energy range of interest for Michel electrons [0, $M_\mu/2$ ($M_\mu = 105$ MeV)] the fractional contributions to the stopping power from ionization versus radiation changes significantly.

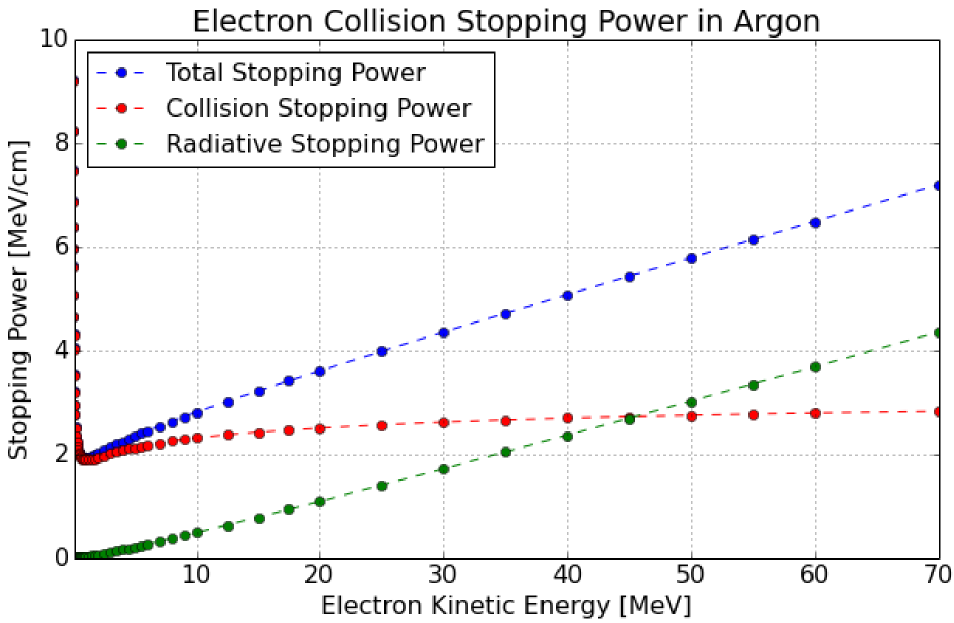

Figure 4: National Institutes of Standard and Technology (NIST) stopping power data for argon [4]. Collision stopping power denotes energy lost by electron ionization. Radiative stopping power indicates the average energy lost to photons via electron Bremsstrahlung.

It is important to note that energy loss via radiative processes occurs via electron Bremsstrahlung, which, unlike ionization charge deposited via collision, consists of the discrete production of often high energy (relative to the electron's energy) photons. While the distribution shown in Fig. 4 shows the average energy loss to radiative processes, case by case the production of photons, and their energy, is a stochastic process.

Photons can travel tens of centimeters in argon before pair-producing. In the case of electrons of order tens of MeV, these distances can be significantly larger than the extent of the inprint left in the detector by ionization charge produced by the decay electron. This has an impact on the ability to collect all charge associated with a Michel electron. We therefore expect that a topological-based charge-clustering algorithm will not be able to successfully collect all charge deposited by the charged products of radiated photons. Due to the significant energy-dependence of the process via which charge is deposited seen in Fig. 4, this will lead to an energy-dependent charge-clustering efficiency.

We take a closer look at how radiative stopping power affects electrons in the tens of MeV energy range. To do so we produce a sample of Monte Carlo electrons in the detector, and use Geant4 to simulate their propagation through the TPC. We then study the truth-level information on the charge deposited and particles produced as the electrons traverse the detector volume.

In Fig. 5 we show, for electrons of different energies, the fraction of the electron's initial energy transferred to photons via electron Bremsstrahlung. From this we can see that the larger the electron energy is, the larger the fraction, on average, of energy transferred to radiative photons. This conclusion is in agreement with what is shown in Fig. 4. Additionally, we can see that for electrons in a given energy range, the distribution of fractional energy lost to radiative photons is very wide. This follows from the stochastic nature of the Bremsstrahlung process.

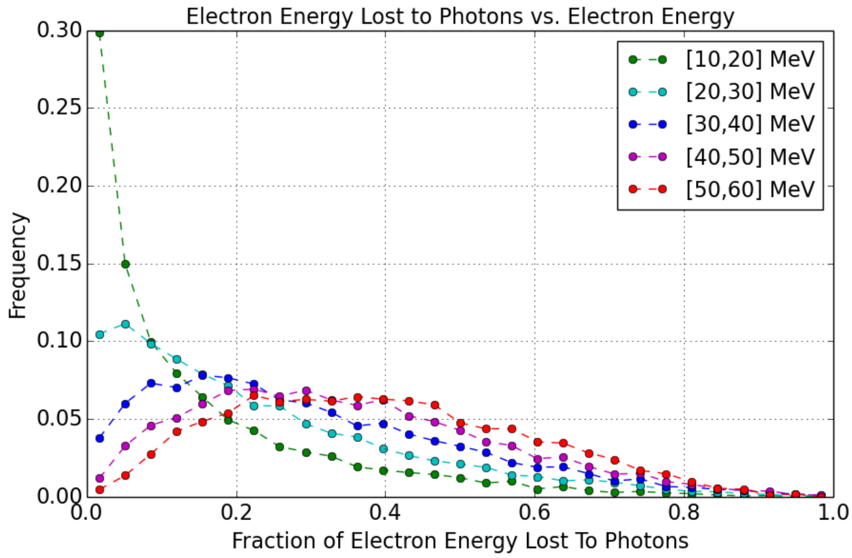

Figure 5: Fraction of an electron's energy lost to radiative processes. For each energy range a large number of electrons was simulated in the detector. For each electron, the fraction of energy transferred to "primary" photons (photons to which energy is transferred directly by the original electron) is calculated. Each curve shows the distribution of such energy transfers for electrons in a given energy range.

Because we rely on information pertaining to the spatial distribution of charge deposited by Michel electrons, and we have shown that photons produced via electron Bremsstrahlung can carry a significant portion of a Michel electron's energy a considerable distance away from the origin of the Michel electron, we are interested in seeing the effect that energy loss due to radiative photons can have on the reconstructed energy spectrum. Fig. 6 shows the charge collected on the TPC collection plane for a sample of Monte Carlo Michel electrons including (red) and excluding (black) the charge that is deposited by the byproducts of radiative photons. These two curves highlight the significant difference between the two extreme scenarios presented. The significant distortion in the distribution, which now presents a rather narrow peak, is the consequence of the energy-dependence of the production of Bremsstrahlung photons. Higher energy Michel electrons will lose more of their energy to photons relative to lower energy ones, causing the different shape in the distribution.

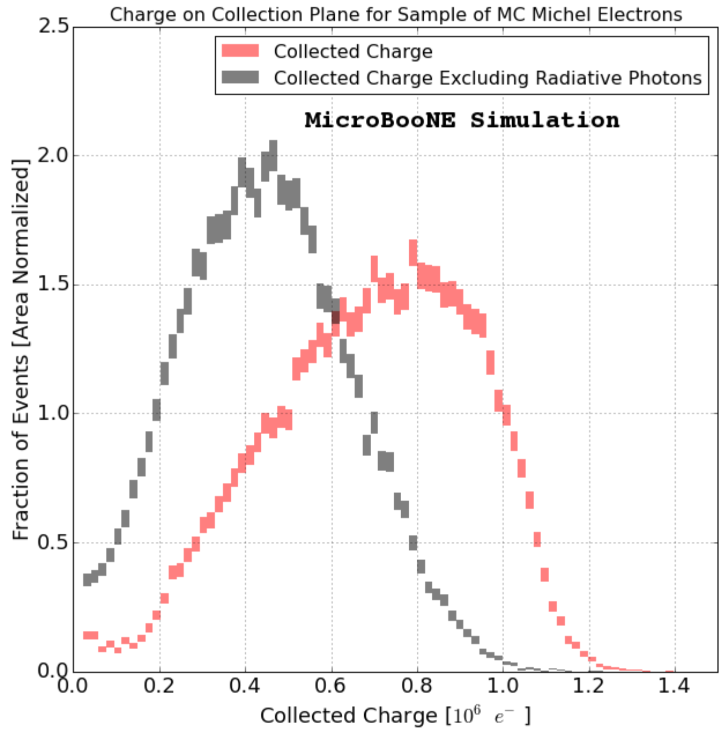

Figure 6: Distribution of charge collected on the TPC collection plane for a sample of Monte Carlo Michel electrons. The two curves show the collected charge when including (red) and excluding (black) the charge that is deposited by the byproducts of radiative photons. The slight rise at very low deposited charge in the distributions is due to Michel electrons that escape the TPC at least in part, and for which only a fraction of their deposited energy drifts to the collection plane.

We conclude this section by stating that Michel electrons are produced in an energy range that is very interesting regarding the physics processes via which electrons lose energy in argon. Across the Michel energy spectrum radiative processes go from being a negligible contribution (at low energies) to the dominant contribution (at higher energies) to the stopping power. Because of the slow drift time in a LAr TPC, the identification of charge associated to different particles must necessarily be done studying the topology and spatial distribution of the charge deposited. Energy transferred to photons, which can travel tens of centimeters before converting and depositing their energy, has an impact on the ability to cluster charge using data from the TPC. This can influece the appearence of a reconstructed Michel electron energy spectrum.

3 Data Samples

The MicroBooNE detector has the ability to read out data by issuing a trigger to the readout electronics. Each time a trigger is issued, 4.8 ms of data from the TPC is recorded and saved. Each 4.8 ms of data associated to a trigger is called an event. In addition to triggering on accelerator-signals associated with the neutrino beam arriving at MicroBooNE, we save a number of off-beam events, triggered by an external pulser or external scintillator strips used to tag cosmic muons. These events are referred to as cosmic events, as they only contain charge deposited by cosmic ray particles entering the TPC. For the analysis presented in this note we only use cosmic events. For each event all data recorded in the 4.8 ms readout window is reconstructed and used to search for potential Michel electrons. A total of 280,751 events were used in this analysis, corresponding to a livetime of 1,347 seconds.

4 Michel Electron Reconstruction and Tagging

We spend this section presenting the method by which we identify Michel electrons in the TPC and collect the charge associated with these particles. Because the drift time of ions in liquid argon is slow compared to the approximately 2 μs muon lifetime, we cannot tag and isolate the charge of an electron produced by a stopping muon simply by separating charge by its arrival time. We instead take advantage of the high-resolution topological and calorimetric information provided by the MicroBooNE TPC to search for signatures in the detector that are characteristic of a stopping muon producing a Michel electron. We use information about the position and charge deposited within the TPC to identify a Bragg peak (due to the increasing energy deposited per unit length of the muon as it comes to a stop) and a kink between the Michel electrn and the stopping muon.

The reconstruction chain begins with an initial signal processing stage, in which the raw signal is deconvolved to account for the detector's field response and electronics shaping time. A noise filter is also applied at this stage. A pulse-finding algorithm is then run on the processed waveforms, to identify and measure the charge deposited on the TPC wires. This step produces reconstructed hits, which carry information on the wire and time of arrival of charge in the detector, as well as an (uncalibrated) measure of the energy deposited in each hit. Hit wire and time information on the collection plane, which is used in this work, represents a 2D top-down projection of charge deposited within the TPC.

Once two dimensional hits have been reconstructed, a clustering algorithm targeted to identify cosmic muons is run to associate together hits that belong to the same particle or interaction. The clustering algorithm takes into account the relative spatial positioning of hits using both wire number and time information in order to decide how charge should be clustered together. These clusters are then provided as input to the topology-specific Michel electron search.

The reconstruction framework developed to tag Michel electrons is detector-agnostic and can be used by other LArTPC detectors for the same purpose. Clusters of hits are provided as input. A series of modularized algorithms is then run on each input cluster to determine if a candidate Michel electron is present in that cluster. If one is found, the hits associated with this candidate Michel electron are grouped together so that they can be used to provide a measure of the energy of the Michel electron. The modularized sequence of algorithms used to identify Michel electrons in the detector allows for a flexible recontruction chain. Each algorithm is designed to calculate specific quantities and act on any values calculated. We will next describe the most significant steps performed within this reconstruction chain.

Hit Sorting and Cluster Profiling As a first step, hits collected within a single cluster are ordered based on their spatial orientation. The ordered list of hits is then used to produce a profile of the cluster's charge deposition as it travels within the detector. The charge profile obtained is subsequently smoothed by averaging charge collected on neighboring hits via a truncated mean algorithm. The resulting charge profile can be used to identify a rise in the charge deposited per unit distance, which can be associated with the Bragg peak of a stopping muon. Additionally, a profile of the local linearity along the cluster is calculated. The measure of the local linearity, per hit, is given by the χ^2 fit value to a line fitted to the coordinates of the hits closest to the hit being examined. This measure of the linearity can be used to identify kinks along the cluster, which can indicate the possible boundary between a muon's stopping point and the outgoing Michel electron.

Bragg Peak Identification As muons come to a stop in the MicroBooNE TPC, their dE/dx will increase, depositing more energy per unit distance traveled. Because neighboring hits associated with a muon traveling in a straght line can be considered as equidistant, the charge measured on hits as the muon comes to a stop will increase. This will lead to a characteristic charge-profile in which a Bragg peak from the stopping muon should be easily identifiable. In order to idenfity a muon's stopping point, we search for a possible Bragg peak in the vicinity of the hit with the most charge in the cluster, and subsequently measure the significance of the charge deposited within the Bragg peak to separate through-going from stopping muons. Fig. 7 shows an event display of a tagged Michel electron from data (top), along with the charge profile calculated along the ordered hits of the cluster (bottom).

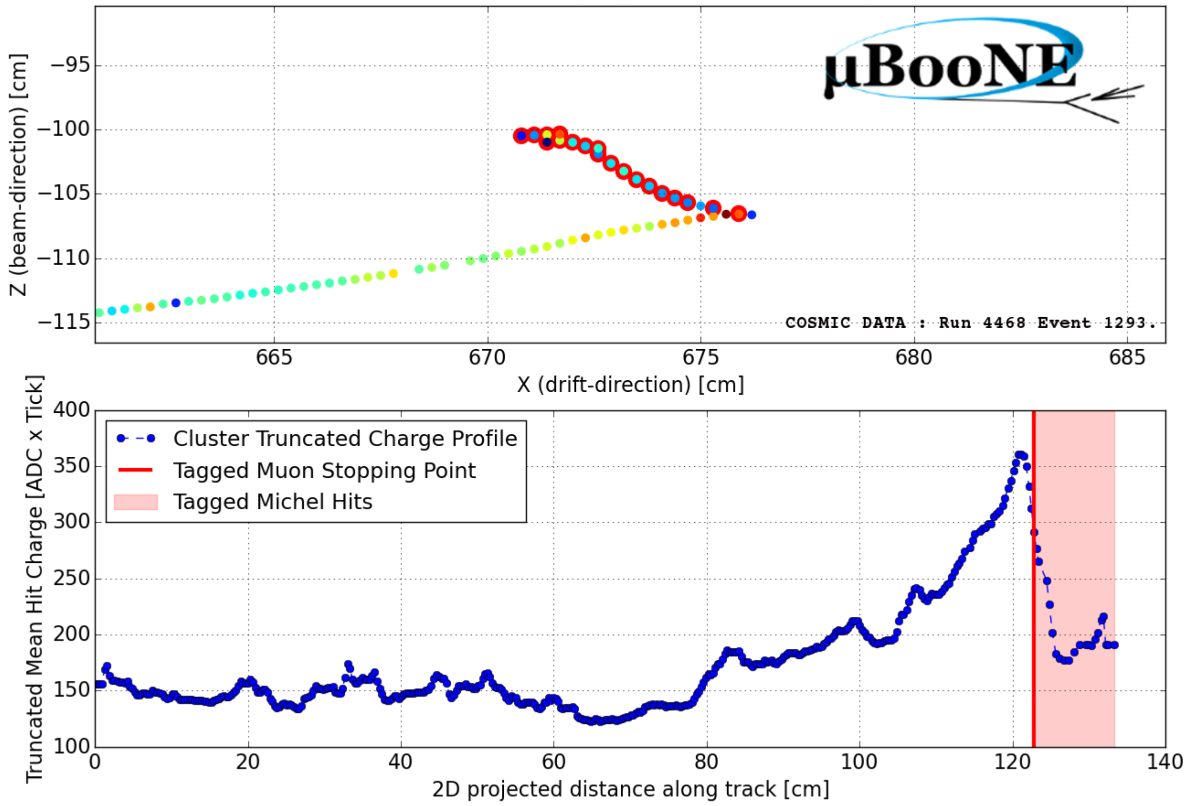

Figure 7: Event display showing the hits associated with a tagged Michel electron (top) and the charge-profile calculated along the ordered list of hits in the cluster (bottom) used within the reconstruction to identify stopping muons. The red vertical line in the bottom figure indicates the location of the identified stopping point for the muon, and the region shaded in red represents the set of hits along the cluster identified as belonging to the candidate Michel electron. In the top panel, the 2D event display shows information in wire vs. time coordinates, with the vertical axis, labeled Z, indicating the position along the wire-plane, and the horizontal, X-axis, indicating the position of each hit in time. Each hit is represented as a circle, with the color indicating the charge measured. Blue indicates lower charge. Hits that are outlined in red represent the hits associated with the tagged Michel electron.

Muon-Michel Kink Identification In addition to requiring the identification of a stopping muon, we subsequently ask that hits which come after the identified stopping point come at an angle with respect to those from the muon track. Requring a kink at the stopping point allows us to improve the purity of our sample. In order to find such a kink, the local linearity measured in the neighborhood of the identified stopping point is measured. A low value to the linearity χ^2 is required in order for a Michel electron to be tagged. Fig. 8 shows an event display associated to a tagged candidate Michel electron from the data. On the bottom half we show the linearity profile along the ordered hits. The red vertical line denotes the tagged position of the stopping muon. A dip in the local linearity at this point can be observed.

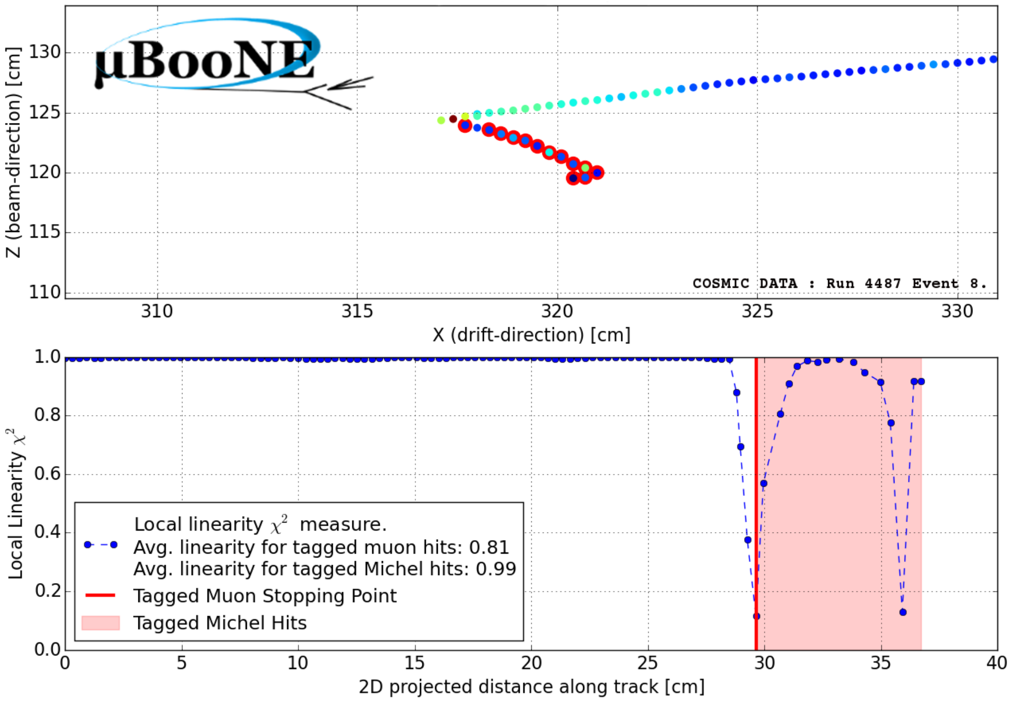

Figure 8: Event display showing the hits associated with a tagged Michel electron (top) and the linearity-profile calculated along the ordered list of hits in the cluster (bottom). The red vertical line in the bottom figure indicates the location of the identified stopping point for the muon, and the region shaded in red represents the set of hits along the cluster identified as belonging to the candidate Michel electron. The local linearity quantity indicates the presence of a kink in coincidence with the identified stopping point. In the top panel, the 2D event display shows information in wire vs. time coordinates, with the vertical axis, labeled Z, indicating the position along the wire-plane, and the horizontal, X-axis, indicating the position of each hit in time. Each hit is represented as a circle, with the color indicating the charge measured. Blue indicates lower charge. Hits that are outlined in red represent the hits associated with the tagged Michel electron.

After the identification of a candidate stopping point for a muon, the list of selected hits tagged as belonging to the candidate Michel electron is refined. We search in the neighborhood of the tagged electron for hits that may have been skipped at the first clustering stage. We additionally apply a series of algorithms aimed at removing potential mis-identified events. This step is performed in order to improve the purity of our sample. In this stage we examine quantities such as the length of the cluster segment associated with the muon, or the angle between the muon segment and the tagged Michel hits. These cuts help us remove potentially mis-identified events.

Finally, two analysis cuts are applied to the sample. Events with a large average charge per hit (for hits associated with the Michel electron) are excluded from consideration. These clusters tend to have a significant amount of charge contamination due to hits from the muon's Bragg peak which have a larger charge, on average, than hits from the Michel electron. For a similar reason, we remove tagged events in which there are many hits associated to the Michel electron located too closely to hits associated with the decaying muom. These cuts target the removal of tagged events in which a Michel electron may have been successfully identified, but which may contain a significant amount of charge contamination from the decaying muon. We apply these cuts in order to end up with a sample that can be used to measure a reliable Michel electron energy spectrum.

We next show some event displays of tagged Michel electrons. Fig. 9 shows several of the tagged Michel electrons found in cosmic events. Each image represents a zoom-in on the hits in the vicinity of a tagged Michel electron and shows the position, in wire-time coordinates, of hits with their associated charge represented by the hit color. Charge increases as the color moves from blue to red. Hits that were tagged as belonging to a Michel electron are outlined in red.

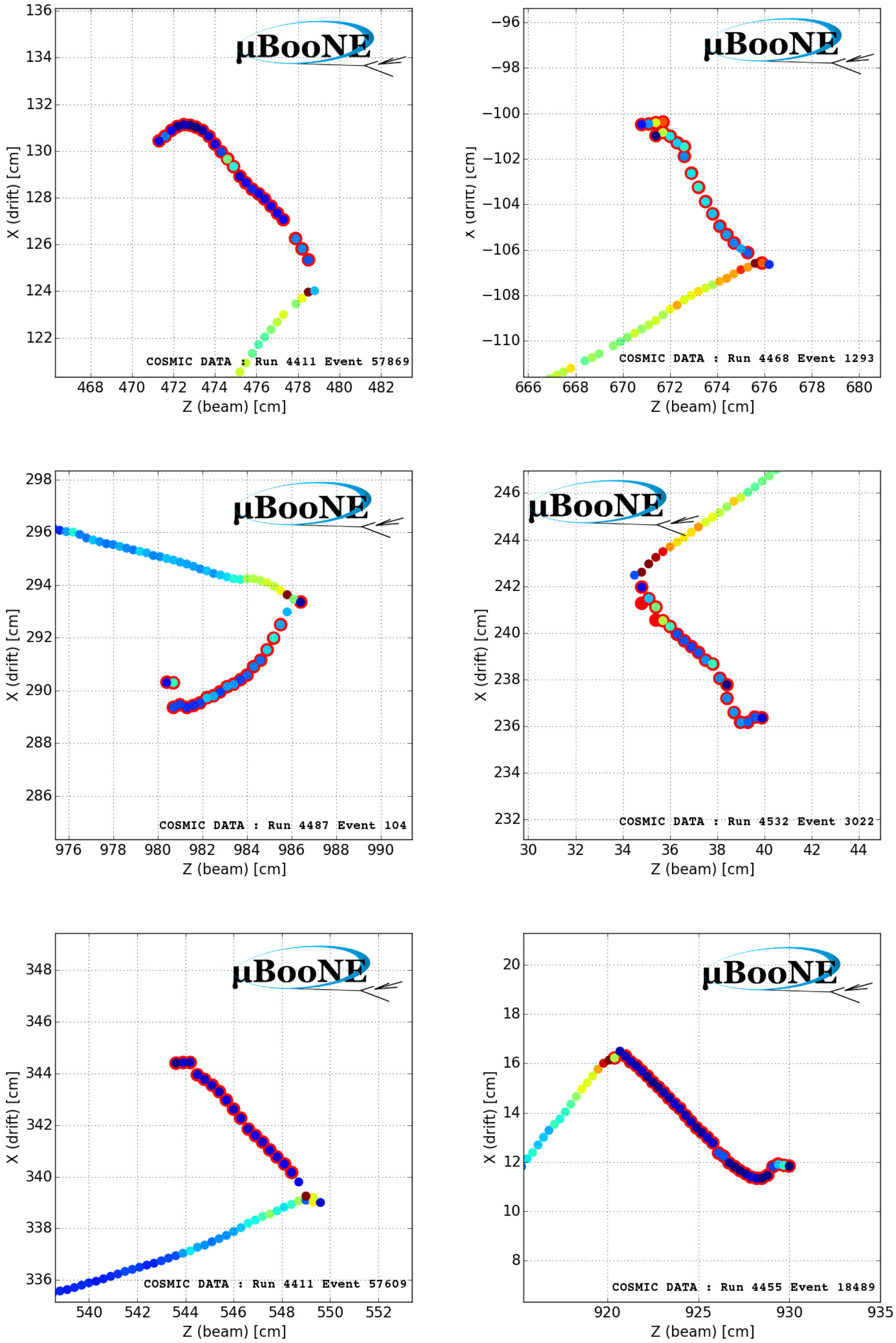

Figure 9: Event displays of tagged Michel electrons from data. Each image shows the reconstructed hits in the wire,time view of the collection plane in the vicinity of a tagged Michel electron. Hit charge (measured in ADC x Tick) is represented by the hit color. Charge increases as the color moves from blue to red. Hits tagged as belonging to a Michel electron are outlined in red.

5 Michel Electron Energy Reconstruction

This chapter will present the process through which the energy of a reconstructed Michel electron is calculated, starting from the pulse integral (measured in ADC x Ticks) of hits associated with a candidate Michel electron. To calculate the energy associated with each Michel electron, we first use a gain calibration constant to convert from hit integral to charge, measured in fC. This calibration constant accounts for the electronics gain and shaping response, digitization, and signal processing. We calculate this quantity using data taken during TPC calibration runs. A pulse of known charge can be sent to each wire in the MicroBooNE TPC. By injecting a pulse of known charge, we can study the detector's electronics response and calculate a calibration gain. We measure an average calibration gain of 36.1 ADC x Ticks / fC of input charge.

Now that we have a measure of the charge drifting to the collection plane associated with each hit, we need to calculate the energy deposited in the TPC which produced the drifting charge. Drifting electrons are produced via ionization of the argon atoms. This process is associated with an ionization work function of 23.6 eV/e^-. Before directly converting from charge to energy, we need to account for two important physical processes that affect our TPC: ion recombination as the argon is ionized by a traversing particle, and charge quenching which occurs as the ionized charge drifts across the TPC.

Recombination Correction Recombination is the process through which ionized electrons will recombine with the positive ions produced along a partcle's trajectory. This physical process is highly dependent on the density of ions and the magnitude of this effect depends both on the amount of energy deposited per unit distance (referred to as dE/dx), as well as the strength of the external electric field which drifts charge towards the TPC wires. In this analysis we model the effects of recombination according to the treatment and results obtained by the ArgoNeuT collaboration [5]. We define the recombination factor, R, as the quenching factor which allows us to go from the amount of energy deposited to the number of drifting electrons produced. This factor is defined in Eq. 2.

$$dQ \times W_{\text{ion}} = dE \times R\left(\frac{dE}{dx}, E_{\text{field}}\right). \tag{2}$$

Where W_{ion} denotes the work function for ionizing an argon atom. This corresponds to 23.6 eV. ArgoNeuT makes use of the Modified Box Model to convert from charge to energy, according to this model we have:

$$\frac{dE}{dx} = \frac{e^{\beta \times \frac{W_{ion}}{e^-}\frac{dQ}{dx}} - \alpha}{\beta} \tag{3}$$

Given equations 2 and 3, we can express the recombination factor R as:

$$R = \frac{ln\left(\frac{dE}{dx} \times \beta + \alpha\right)}{\frac{dE}{dx} \times \beta} \tag{4}$$

With constants α and β given by:

$$\alpha = 0.93 \tag{5}$$

$$\beta = \frac{k_b}{\rho[\text{g/cm}^3] \times E_{\text{field}}[\text{kV/cm}]} \tag{6}$$

$$k_b = 0.212 \tag{7}$$

With ρ denoting the density of liquid argon and E_{field} the strength of the electric field in the TPC, and the values of α and k_b coming from ArgoNeuT's results.
With this information we show in Fig. 10 the value of the recombination factor as a function of dE/dx. We highlight in gray the range of dE/dx values of interest for Michel electrons.

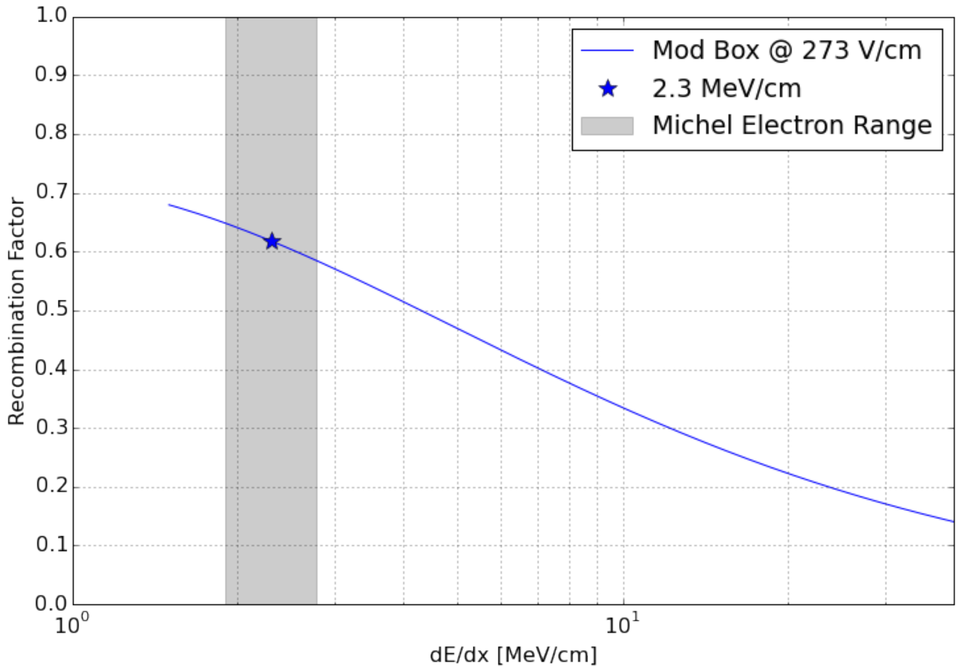

Figure 10: Recombination factor as a function of dE/dx calculated using the Modified Box model as described by ArgoNeuT [5].

Because the reconstruction algorithm we use relies only on 2D collection-plane information, the exact distance between consecutive hits of deposited charge is not known, and we can only measure the projecton on the (x,z) plane, in detector coordinates. This means that our attempt to measure dQ/dx will induce a non-negligible amount of smearing. For this reason, in this analysis we apply a constant recombination factor corresponding to a dE/dx value of 2.3 MeV/cm, which leads to a recombination factor of 0.62.

In future analyses we will be also including other recombination models to evaluate the effect of ion recombination. Additionally, currently efforts are underway within the MicroBooNE collaboration to derive MicroBooNE specific recombination parameters to the various recombination models.

Lifetime Correction As electrons drift towards the wire-plane, they will be absorbed by impurities in the liquid argon. The constant cross-section for absorption as electrons travel in the argon leads to an absorption probability that is exponential with the total drift time. The quenching factor due to impurities in the argon can be quantified by a single parameter, the ionization electron lifetime, τ. Given the electron lifetime, the charge reaching the wire-plane, in relation to that produced as ionization electrons, is given by Eq. 8.

$$Q = Q_0 \times e^{-t/\tau} \tag{8}$$

In order to appropriately correct for the electron lifetime quenching, we must know the drift time of charge collected on the wire-plane. The arrival time of charge recorded by the electronics is equal to the time at which the charge was deposited with respect to the trigger time, plus the drift time required to reach the wire plane. The recorded information from the TPC is therefore not enough to infer the true drift time. Charge which enters the detector very close to the wire-plane later in the readout window will be collected at the same time as charge deposited early on in the readout window, but far away from the anode. This causes an ambiguity that cannot be resolved without using the true arrival time inferred from associating the drifting charge with the corresponding signature in MicroBooNE's optical detectors. Because we do not attempt to perform this reconstruction step in this analysis, we do not know the arrival time of the charge associated with candidate Michel electrons. Instead of correcting for the lifetime event-by-event, we therefore apply a constant correction factor to account for electron quenching due to lifetime. We take this constant factor to be the average correction factor for charge deposited uniformly in the TPC's drift coordinate. Given an electron lifetime τ of 8 ms, the anode-cathode 2.56 meter separation, and the electron drift velocity in MicroBooNE of 1103 m/s (see Ref. [6]), we calculate an electron-lifetime correction factor by integrating the inverse of Eq. 8 over all drift, positions, and averaging. This calculation is carried out in Eq. 9.

$$f_{\text{lifetime}} = \frac{1}{T_{\text{drift}}} \int_{t=0}^{t=T_{\text{drift}}} e^{t/\tau} dt = \frac{1}{2.32\ ms} \int_{t=0\ ms}^{t=2.32\ ms} e^{t/8\ ms} dt = 1.16 \tag{9}$$

We can now convert the measured charge collected by the TPC to the amount of energy deposited by a Michel electron. We do this according to Eq. 10. The constant factors applied for the lifetime correction and recombination effect contribute on the order of 10% to the smearing energy resolution.

$$\mathrm{E(MeV)} = \mathrm{Q(e^-)} \times \frac{23.6}{10^6} \left[\frac{MeV}{e^-}\right] \times 1.16[\text{Lifetime Corr.}] \times \frac{1}{0.62}[\text{Recombination Corr.}] \tag{10}$$

Given Eq. 10, We produce an energy spectrum measured on an MeV scale. We show in Fig. 11 the reconstructed Michel electron energy spectrum, for the same events tagged as candidate Michel electrons identified by the method described in Sec. 4.

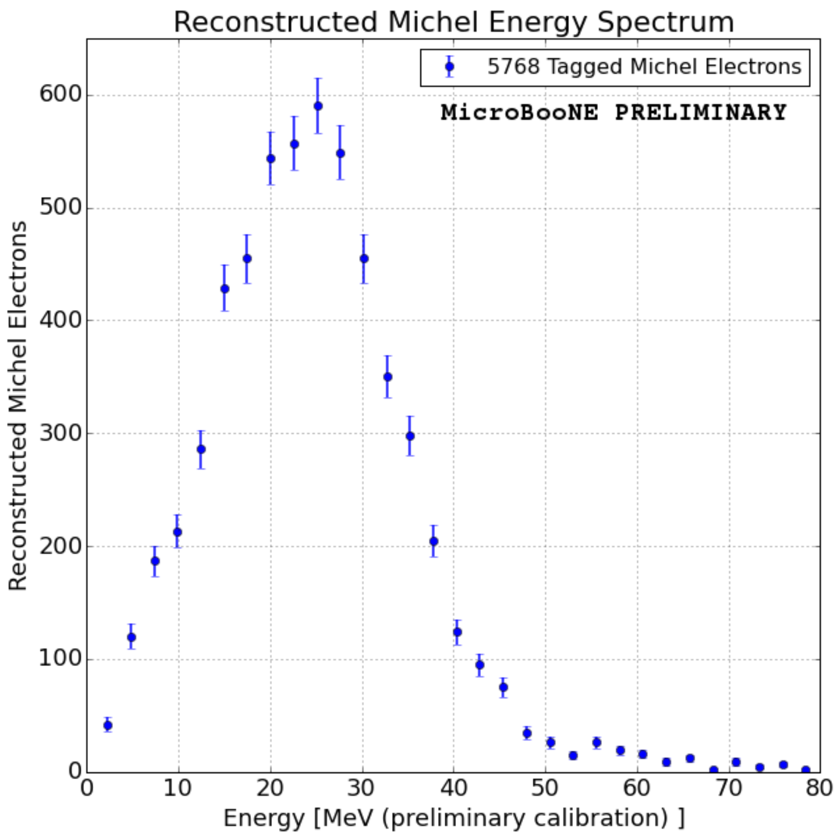

Figure 11: Reconstructed Michel electron Energy Spectrum produced using cosmic data taken with the MicroBooNE detector. Error bars represent statistical uncertainties only.

We can compare the reconstructed energy spectrum we obtain from data with what we expect to see from Monte Carlo. Given the reconstructed spectrum shown in Fig. 11 we overlay it on the expected spectrum obtained by looking at Monte Carlo data. In this comparison, we look at two extreme cases: one in which all Michel electron energy is successfully collected, and another in which all charge deposited by electrons produced by radiative photons escapes detection. In addition, to mimic the effects of the energy reconstruction applied to the data we take the truth energy collected at the collection plane, and apply the same conversion factor in Eq. 10 to convert to an MeV scale. Fig. 12 thus shows the reconstructed energy spectrum from data (blue), overlayed on the calculated energy spectrum from Monte Carlo assuming all charge associated with a Michel electron is successfully collected (red), as well as under the assumption that all energy transferred to radiative photons escapes detection (black). We notice that the reconstructed spectrum from data falls inbetween the two extreme cases, indicating that the reconstruction algorithm we apply is identifying a portion of the charge transferred to radiative photons, likely associated to photons that travel a shorter distance before pair-producing.

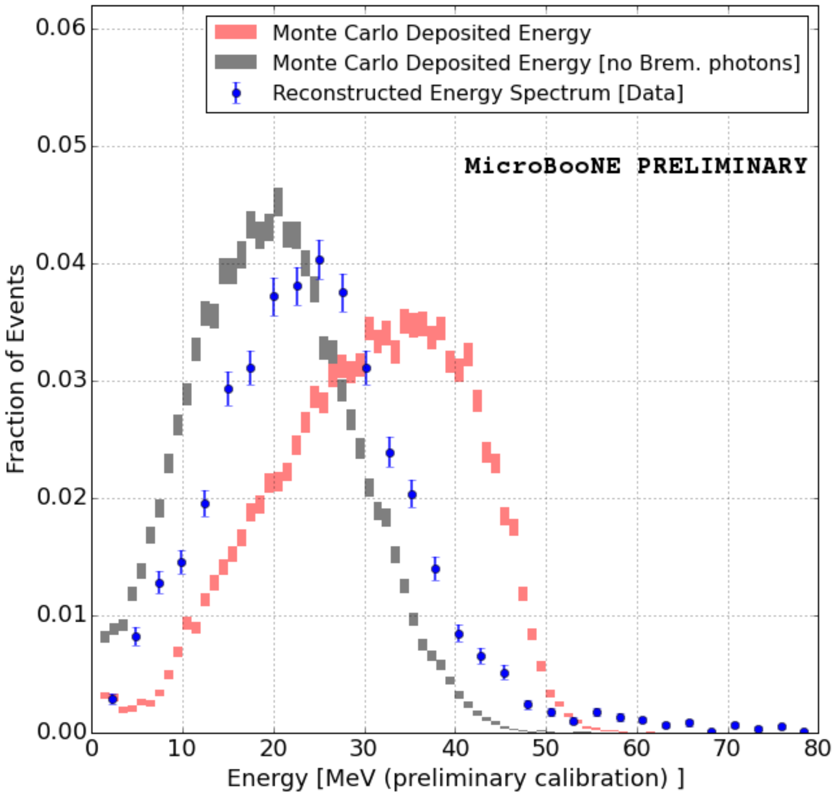

Figure 12: Reconstructed Michel electron Energy Spectrum produced using cosmic data taken with the MicroBooNE detector (blue). We additionally show the energy spectrum produced using a Monte Carlo sample of Michel electrons, for which the truth charge collected at the collection plane is converted to an energy scale applying the same conversion as for the data. We show two Monte Carlo distributions, indicating the extreme scenarios concerning our ability to cluster charge deposited by Michel electrons. In red we show the energy calculated assuming all charge deposited by a Michel electron is successfully collected, while in black we show the same distribution under the assumption that all charge released to radiative photons escapes detection. Each curve is area normalized. Error bars represent statistical uncertainties only. Each curve is normalized to an area equal to one.

We conclude this section by comparing the energy spectrum reconstructed from data (shown in Fig. 11) to that obtained following the same reconstruction procedure on Monte Carlo. The two spectra are shown overlayed in Fig. 13. The reasonable agreement between the two samples indicates that we understand our modeling of Michel electrons in the TPC. We are working on improving our energy calibration by using a sample of cosmic muons to provide channel-by-channel gain measurements. These changes may help address the slight shift in the overall energy scale which can be seen in the data and monte-carlo distributions.

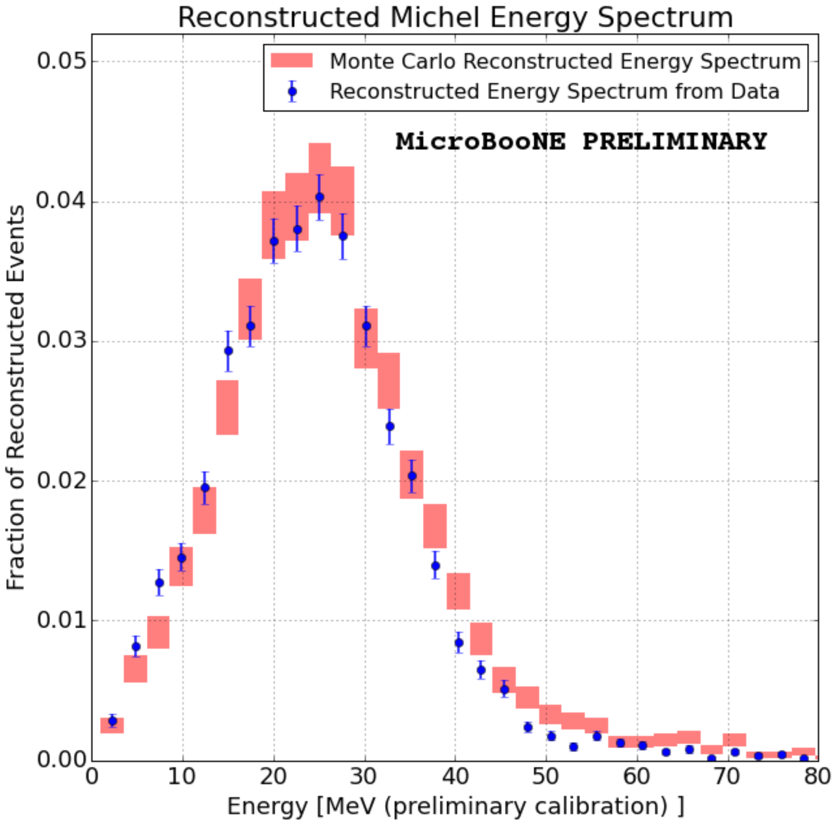

Figure 13: Reconstructed Energy spectrum from cosmic data (blue data points) overlayed on the energy spectrum reconstructed from Monte Carlo (red bands) following the same procedure as for the data. Each curve is area normalized to one. Error bars represent statistical uncertainties only.

6 Conclusion

We have developed a reconstruction framework aimed at searching for Michel electrons from 2D TPC data from the MicroBooNE detector. The algorithm developed searches for Michel electrons by looking at clustered hits, sorting them based on their spatial orientation, and searching for a Bragg peak and kink indicative of a stopping muon producing a Michel electron. We have run this algorithm on a large data sample of 280 thousand cosmic events, finding over 5 thousand Michel electron candidates. We have thus demonstrated that we can successfully employ the calorimetric and topological information provided by the MicroBooNE TPC to identify Michel electrons produced within a sample of cosmic events. We have measured an electronics gain factor as well as calibration constants to calculate an energy scale, accounting for the settings of the MicroBooNE electronics and the recombination and lifetime effects on charge deposited in the TPC. We were then able to produce a Michel energy spectrum, shown in Fig. 11. The spectrum obtained agrees with what one would expect, once the energy loss to radiative photons is accounted for. We notice that the employment of a 2D reconstruction algorithm introduces a smearing of the reconstructed energy due to the constant recombination and electron-lifetime correction factors applied. Furthermore, we note that a 3D clustering algorithm could further improve our ability to successfully cluster charge deposited by Michel electrons, and specifically the energy radiated away via Bremsstrahlung photons. With this work we show that for electrons in the tens of MeV energy range the loss of energy to radiative photons is an important factor that needs to be carefully considered when performing an energy measurement.

References

[1] The Particle Data Group
PDG Summary Tables
`http://pdg.lbl.gov/2015/tables/rpp2015-sum-leptons.pdf`
2015

[2] The MicroBooNE Collaboration
MicroBooNE Technical Design Report
`http://www-microboone.fnal.gov/publications/TDRCD3.pdf`
2012

[3] Marcel Bardon, et. al.,
Measurement of the Momentum Spectrum of Positrons from Muon Decay
`PRL, 14, 449 (1965)`
`http://journals.aps.org/prl/pdf/10.1103/PhysRevLett.14.449`

[4] National Institutes of Standards and Technology
ESTAR : Stopping-Power and Range Tables for Electrons
`http://physics.nist.gov/PhysRefData/Star/Text/ESTAR.html`

[5] R. Acciari, et. al.
A study of electron recombination using highly ionizing particles in the ArgoNeuT Liquid Argon TPC
`Journal of Instrumentation (JINST), Vol 8, P08005` `http://arxiv.org/abs/1306.1712`
June 2013.

[6] The MicroBooNE Collaboration
Measurement of the Average Drift Velocity Utilizing UV Laser Data
`MICROBOONE-NOTE-1009-PUB`
April 2016.